

Figure S1

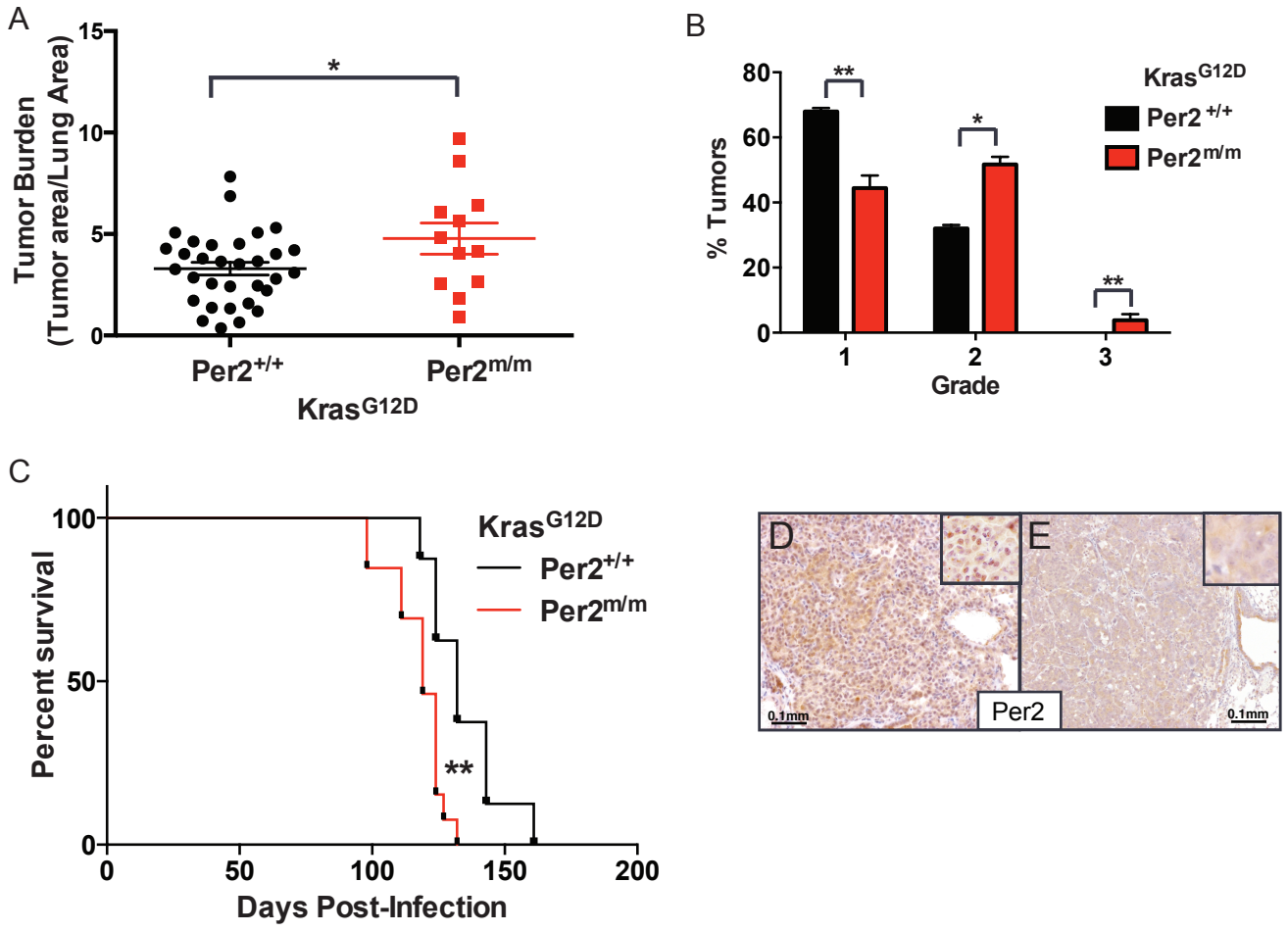


Figure S1, related to Figure 1. Characterizing the effects of circadian rhythm disruption on lung tumorigenesis. Histological analysis of lung tumor burden (**A**) and grade (**B**) in K mice with WT ($Per2^{+/+}$) or mutant ($Per2^{m/m}$) $Per2$. (**C**) Kaplan-Meier survival analysis for K animals with WT ($Per2^{+/+}$) (n=8) or mutant ($Per2^{m/m}$) $Per2$ (n=13). Immunohistochemical analysis of $Per2$ in $Per2^{+/+}$ (**D**) and $Per2^{m/m}$ (**E**), insets contain high magnification images, scale bar=0.1mm. Note: * = $p < 0.05$, ** = $p < 0.01$, *** = $p < 0.001$. To obtain p values, Log-rank (Mantel-Cox) test was performed for Kaplan-Meier survival and two-sided Student's t-test was performed for histological analyses of tumor burden, grade and number.

Figure S2

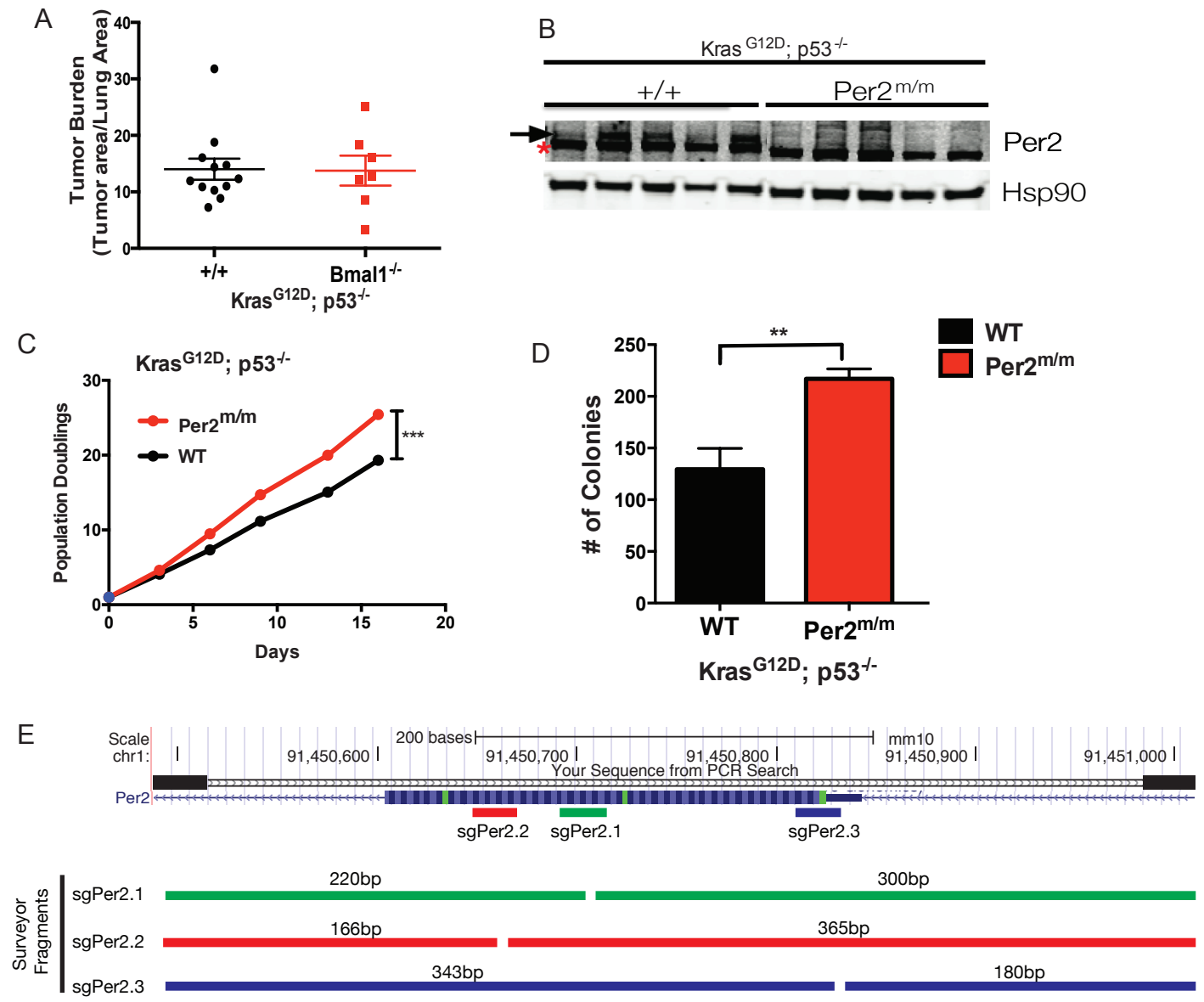


Figure S2, related to Figure 2. Cell autonomous effects of GEMM-derived cell lines from circadian mutants. (A) Histological analysis of lung tumor burden in KP tumors with tumor-specific loss of *Bmal1* (*Bmal1^{Δ/Δ}*) (n=7) compared to WT controls (*Bmal1^{+/+}*) (n=12). (B) Western blot analysis of GEMM-derived KP cell lines from wildtype (+/+) or mutant (*Per2^{m/m}*) *Per2*, arrow indicates *Per2* band, asterisk indicates non-specific band, western blot image partially cropped between WT and *Per2^{m/m}* lanes to remove lanes from samples not pertinent to this study. Functional assays for KP cell lines with WT (+/+) or mutant (*Per2^{m/m}*) *Per2*: (C) Population Doublings analysis, (D) low-density colony formation assay. (E) Schematic of the amplicon (Snapshot from UCSC genome-browser) used for Surveyor analysis containing the first coding exon of *Per2* and the binding location of the three short-guide RNAs tested in this study. Bottom of schematic illustrates the expected band sizes seen in Surveyor if there is CRISPR/Cas9-editing at the locus in the present of each sgRNA targeting *Per2*. Note: ** = p<0.01, *** = p<0.001, obtained from two-sided Student's t-test. All error bars denote standard deviations.

Figure S3

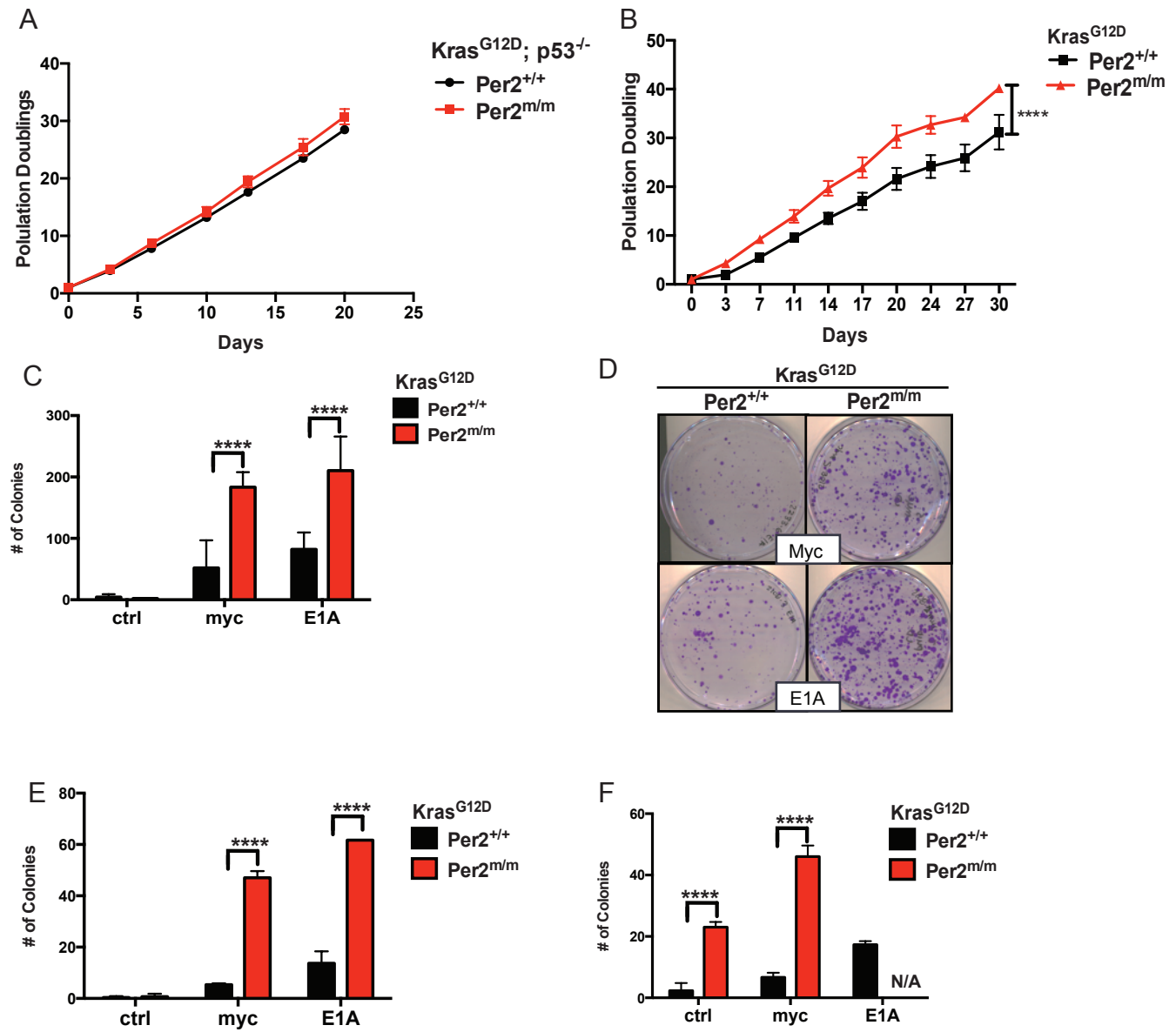


Figure S3, related to Figure 2. Cell autonomous effects of Per2 loss in MEFs. Functional characterization of K and KP MEFs with WT (+/+) or mutant (*Per2^{mm}*) *Per2*: **(A)** Population doublings of KP MEFs; **(B)** Population doublings of K MEFs; **(C)** Colony numbers from low-density clonogenicity assays; **(D)** Representative images of low-density assays; **(E)** colony numbers from 3D agar assays and **(F)** colony numbers from high-density growth assays, N/A: increased growth no colonies could be measured. All experiments represent data from three independent experimental replicates from 3 independent MEF lines. Note: **** = $p < 0.0001$, obtained from two-sided Student's t-test. All error bars denote standard deviations.

Figure S4

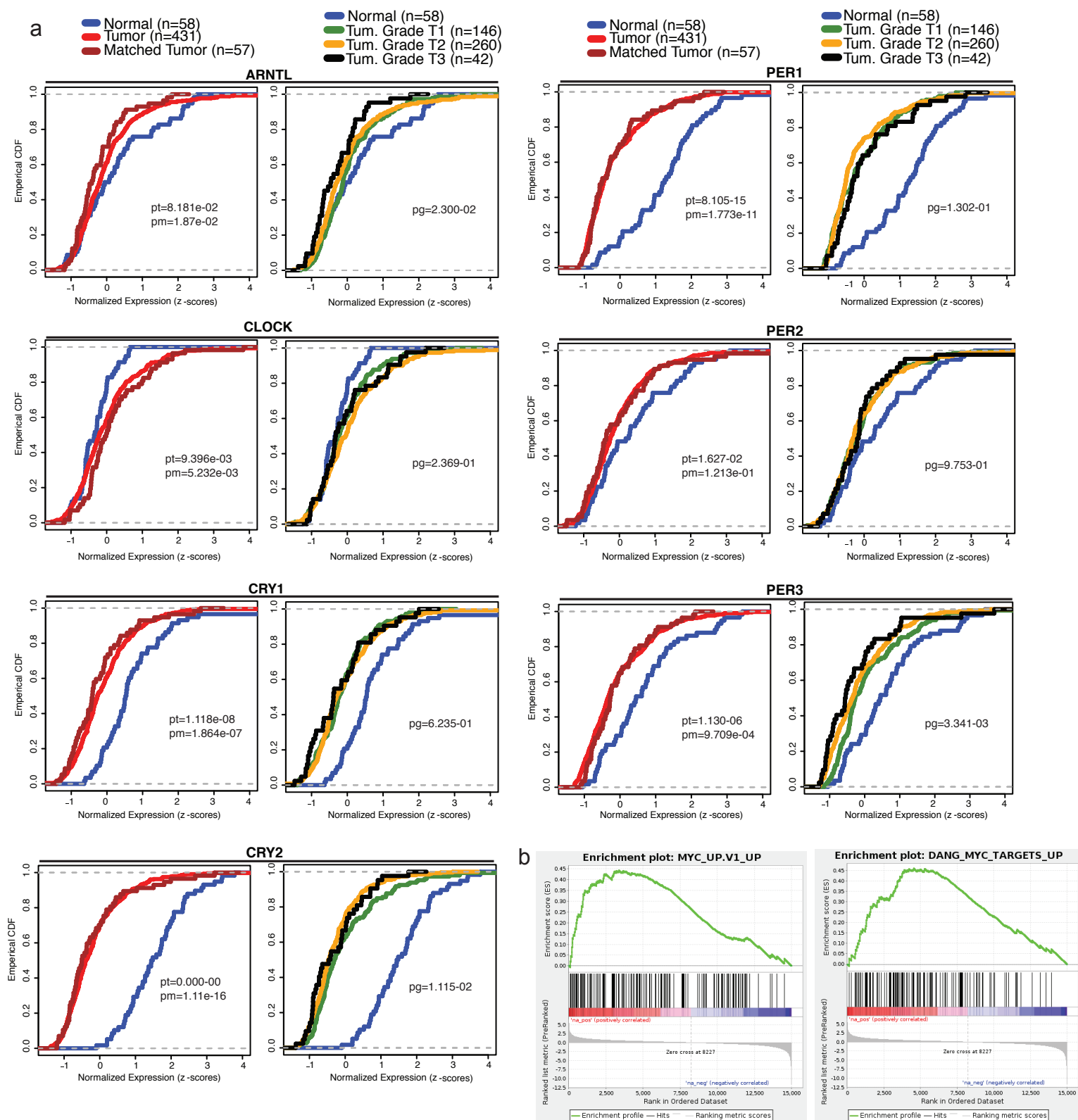


Figure S4, related to Figure 3. Gene expression analysis of core circadian genes in human lung adenocarcinoma. (A) Cumulative Distribution Function (CDF) plots comparing the expression of circadian genes (left panel) in TCGA lung adenocarcinoma normal lung (n=58), matched tumor (n=57), and all tumor samples (n=431). Analysis of circadian gene expression across tumor grades (right panel). p-values shown in each plot: p_m = p-value of differential expression between normal samples and matched tumors (Kolmogorov Smirnov test); p_t = p-value of differential expression between normal samples and all non-matched tumors (Kolmogorov Smirnov test); p_g = p-value of differential expression between tumor grades I, II, III (Kruskal Wallis test). **(B)** MYC GSEA genesets enriched in human tumors with low PER2 expression within the low PER2 versus high PER2 expression signature.

Supplemental Experimental Procedures

Histology and Immunohistochemistry

Mice were euthanized by carbon dioxide asphyxiation. Lungs were perfused through the trachea with 4% paraformaldehyde (PFA), fixed overnight, transferred to 70% ethanol and subsequently embedded in paraffin. Sections were cut at a thickness of four micrometers and stained with H&E for pathological examination. Immunohistochemistry (IHC) was performed on a Thermo Autostainer 360 machine. Slides were antigen retrieved using Thermo citrate buffer, pH 6.0 in the Pretreatment Module. Sections were treated with Biocare rodent block, primary antibody, and anti-Mouse (Biocare), anti-Rabbit (Vector Labs) or anti-rat (Vector Labs) HRP-polymer. The slides were developed with Thermo Ultra DAB and counterstained with hematoxylin in a Thermo Gemini stainer and coverslipped using the Thermo Consul cover slipper. The following antibodies were used for IHC: anti-Per2 (Alpha Diagnostics, PER21-A, 1:1,200), anti-BrdU (Abcam, 6326, 1:100), anti-c-myc (Abcam, Ab32072, 1:50). All pictures were obtained using a Nikon 80i microscope with a DS-U3 camera and NIS-elements software.

Total lung area occupied by tumor was measured on hematoxylin and eosin (H&E) stained slides using NIS-elements software. Histopathological grading of tumor was performed with the assistance of Dr. Roderick Bronson. Quantitation of BrdU and c-Myc positive nuclei was performed using ImageJ using tumors of the same histological grade.

Cell culture experiments

Early passage MEFs (p3-4) were used for all experiments. *Kras*^{LSL-G12D/+}; *p53*^{flox/flox} (KP) or *Kras*^{LSL-G12D/+} (K) MEFs with WT or mutant *Per2* (*Per2*^{m/m}) were isolated from embryonic day 14.5 (E14.5) littermates. MEFs were on a mixed 129 Sv/C57BL/6 background. MEFs were infected with high titer adenovirus expressing Cre to induce the K and KP mutations. Tumor-derived lung cancer cell lines were isolated from grade 3 tumors from KP WT or *Per2*^{m/m} tumor-bearing littermate animals, according to previously described methods (DuPage et al., 2009). LentiCRISPR infected KP C57BL/6 cells were selected with Puromycin and analyzed as a population for protein and surveyor assays.

KP lung cancer cells were grown in 10% FCS/DMEM MEFs were grown as previously described (Tuveson et al., 2004). Population doublings, focus formation, soft agar and subcutaneous transplants in immunocompromised animals were performed as previously described (Tuveson et al., 2004). EdU incorporation was performed using Click-iT EdU Alexa Fluor 647 Imaging kit (Life Technologies, C10340) followed by flow cytometry based EdU quantitation using a Guava flow cytometer (Millipore). For metabolite labeling studies, cells were cultured for 24 hr in DMEM containing 17.5 mmol/L [¹³C] glucose (Cambridge Isotopes Laboratories) prior to metabolite extraction.

Metabolite measurement

For GC-MS, dried metabolites were dissolved in 10 μ L/10 mg wet tissue weight of 2% methoxyamine hydrochloride in pyridine (Sigma) and held at 37°C for 1.5 hr; norvaline was added as an injection control. Tert-butyldimethylsilyl derivatization was initiated by adding 15 μ L/10 mg wet weight of N-methyl-N-(tert-butyldimethylsilyl)trifluoroacetamide + 1% tert-butyldimethylchlorosilane (Sigma) and incubated at 37°C for 1 hr. GC-MS analysis was performed using an Agilent 7890 GC equipped with 30 m DB-35MS capillary column connected to an Agilent 5975B MS operating under electron impact ionization at 70eV with helium as a carrier gas and the detector in scanning mode. MIDs were corrected for natural isotope

abundance as previously reported (Davidson et al., 2016). Glucose, lactate, glutamine, and glutamate were measured using YSI biochemistry analyzer (Yellow Springs Instruments). Exponential growth over the culture period was assumed for flux calculations.

Lentiviral production

Lentiviruses were produced by co-transfection of 293T cells with lentiviral backbone constructs and packaging vectors (delta8.2 and VSV-G) using TransIT-LT1 (Mirus Bio). Supernatant was collected 48 and 72 hours post-transfection, concentrated by ultracentrifugation at 25,000 RPM for 90 minutes and resuspended in an appropriate volume of OptiMEM (Gibco).

Lentiviral vectors and sgRNA cloning

For CRISPR experiments the lentiCRISPR lentiviral vector was used (Shalem et al., 2014). Detailed protocol can be found in prior studies (Ran et al., 2013). For sgRNA cloning, the lentiCRISPR vector was digested with BsmBI and ligated with BsmBI-compatible annealed oligos for sgRNAs against the *Per2*:

sgPer2.1: sense 5'-CACCGGAGCAGTTCTCGTTTCCGC-3', antisense 5'-AAACGCGGAAACGAGAAGTCTCC-3'; sgPer2.2 sense 5'-CACCGCAGTGACTGCGACGACAAT-3', antisense 5'-AAACATTGTCGTCGAGTCACTGC-3'; sgPer2.3 sense 5'-CACCTATCCATTTCATGTCGGGCTC-3', antisense 5'-AAACGAGCCCGACATGAATGGATA-3'
Non-targeting control sgRNA (ctrl): sense 5'-CACCGGCCACGAGTTCGAGATCGA-3', sense 5'-AAACTCGATCTCGAACTCGTGGCC-3'.

Immunoblotting

Cells were lysed with ice-cold RIPA buffer (Pierce, #89900) supplemented with 1× Complete Mini inhibitor mixture (Roche, #11 836 153 001) and mixed on a rotator at 4° C for 30 minutes. Protein concentration of the cell lysates was quantified using the Bio-Rad DC Protein Assay (Catalog #500-0114). 50–80 µg of total protein was separated on 4–12% Bis-Tris gradient gels (Life Technologies) by SDS-PAGE and then transferred to nitrocellulose membranes. The following antibodies were used for immunoblotting: anti-Hsp90 (BD, #610418, 1:10,000), anti-Per2 (Alpha Diagnostics, PER21-A, 1:1,000) and a custom Per2 antibody provided from Cheng C. Lee.

Genomic DNA isolation and Surveyor assay

Genomic DNA from cells was isolated using the High Pure PCR Template Preparation Kit (Roche) following manufacturer guidelines. PCR products for surveyor assay were amplified using Herculase II Fusion DNA polymerase (Agilent), gel purified and subsequently assayed with the Surveyor Mutation Detection Kit (Transgenomic). DNA was separated on 4-20% Novex TBE Gels (Life Technologies) and stained with ethidium bromide. Primers to amplify edited *Per2* locus:

Forward 5'-TTAAGAAGTACTGCCATCCTGCAAGTC-3'

Reverse 5'-ATCAAGAACACATAAACTACTACAGTA-3'

Detailed protocol can be found in prior studies (Ran et al., 2013).

Computational methods summary

For circadian gene expression analyses in TCGA lung adenocarcinoma human tumors, RNAseq expression and clinical annotation datasets were obtained from the Firehose repository (gdac.broadinstitute.org, RNAseqV2). Gene expression levels were compared between normal, matched tumor, and all remaining tumor samples where RNAseq data was available. All computations were performed in the R statistical computing environment (<http://www.R-project.org>). Significance of expression differences was determined using the Kolmogorov-Smirnov test. Differential expression based on tumor grade was assessed using the Kruskal-Wallis test. A differential gene expression signature between the top and bottom 25% of tumors stratified by standardized *Per2* expression levels was determined using Independent Component Analysis (manuscript in preparation). Subsequent gene set enrichment analysis was performed using Gene Set Enrichment Analysis (GSEA) (Mootha et al., 2003; Subramanian et al., 2005) on genes ranked by their correlation with the signature pattern.

Supplemental References

- Davidson, S.M., Papagiannakopoulos, T., Olenchock, B.A., Heyman, J.E., Keibler, M.A., Luengo, A., Bauer, M.R., Jha, A.K., O'Brien, J.P., Pierce, K.A., et al. (2016). Environment Impacts the Metabolic Dependencies of Ras-Driven Non-Small Cell Lung Cancer. *Cell metabolism* 23, 517-528.
- DuPage, M., Dooley, A.L., and Jacks, T. (2009). Conditional mouse lung cancer models using adenoviral or lentiviral delivery of Cre recombinase. *Nat. Protocols* 4, 1064-1072.
- Mootha, V.K., Lindgren, C.M., Eriksson, K.F., Subramanian, A., Sihag, S., Lehar, J., Puigserver, P., Carlsson, E., Ridderstrale, M., Laurila, E., et al. (2003). PGC-1alpha-responsive genes involved in oxidative phosphorylation are coordinately downregulated in human diabetes. *Nature genetics* 34, 267-273.
- Ran, F.A., Hsu, P.D., Wright, J., Agarwala, V., Scott, D.A., and Zhang, F. (2013). Genome engineering using the CRISPR-Cas9 system. *Nat Protoc* 8, 2281-2308.
- Shalem, O., Sanjana, N.E., Hartenian, E., Shi, X., Scott, D.A., Mikkelsen, T.S., Heckl, D., Ebert, B.L., Root, D.E., Doench, J.G., et al. (2014). Genome-scale CRISPR-Cas9 knockout screening in human cells. *Science* 343, 84-87.
- Subramanian, A., Tamayo, P., Mootha, V.K., Mukherjee, S., Ebert, B.L., Gillette, M.A., Paulovich, A., Pomeroy, S.L., Golub, T.R., Lander, E.S., et al. (2005). Gene set enrichment analysis: a knowledge-based approach for interpreting genome-wide expression profiles. *Proc Natl Acad Sci U S A* 102, 15545-15550.
- Tuveson, D.A., Shaw, A.T., Willis, N.A., Silver, D.P., Jackson, E.L., Chang, S., Mercer, K.L., Grochow, R., Hock, H., Crowley, D., et al. (2004). Endogenous oncogenic K-ras(G12D) stimulates proliferation and widespread neoplastic and developmental defects. *Cancer Cell* 5, 375-387.